Supporting Information

A porous metal-organic framework formed by a V-shaped ligand and Zn(II) ion with highly selective sensing for nitroaromatic explosives

Hongming He,[a] Yang Song,[a] Fuxing Sun,[a] Zheng Bian,[b] Lianxun Gao[b] and Guangshan Zhu[a*]*

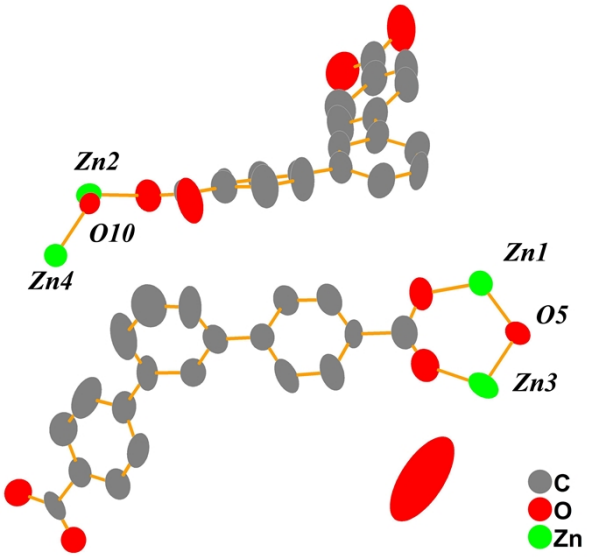

Fig. S1 The asymmetric unit of **JUC-135**.

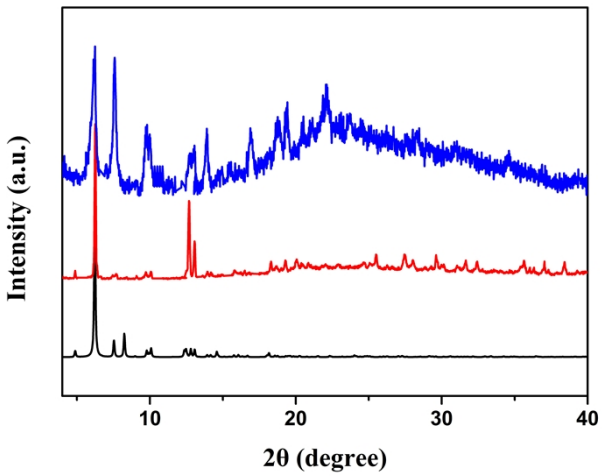

Fig. S2 PXRD of simulated (black), as-synthesized (red) and activated samples (blue) of **JUC-135**.

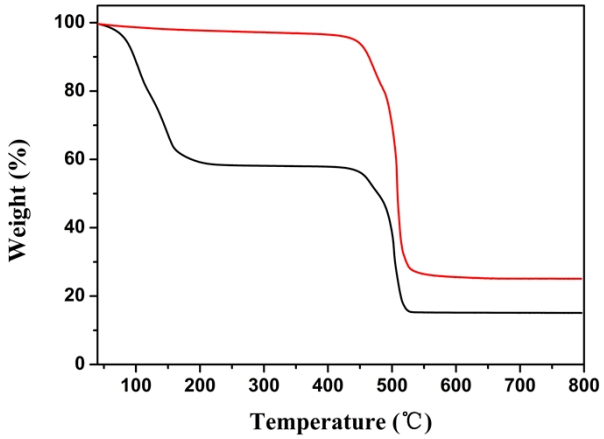

Fig. S3 TGA plots of **JUC-135** (black) and activated **JUC-135** (red) in air condition.

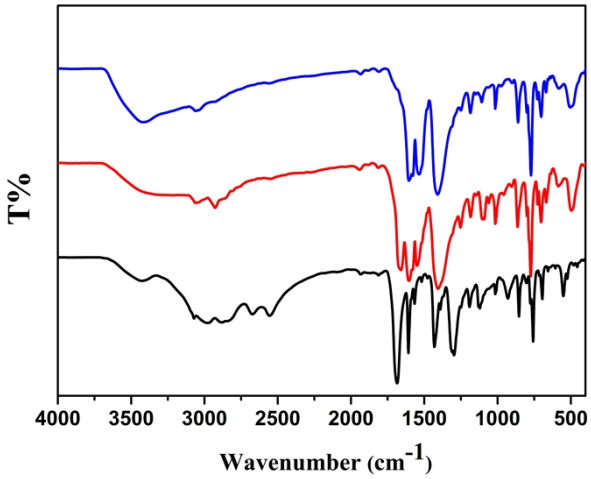

Fig. S4 FT-IR spectra of **H_2DCPB** (black), **JUC-135** (red) and activated **JUC-135** (blue).The characteristic peak of carbonyl asymmetric stretching band (C=O) of –COOH at 1687 cm^{-1} was only found in the black curve, implying that all carboxyl groups of ligand are deprotonated. Meanwhile, the characteristic peak of C=O of DMF molecules at 1662 cm^{-1} is disappeared in the activated sample, implying that all DMF guest molecules are removed completely.

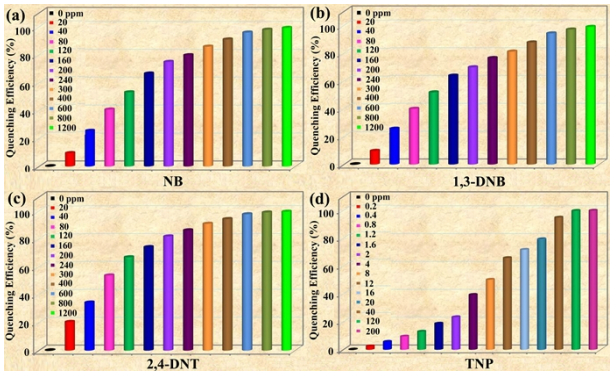

Fig. S5 Corresponding quenching efficiency of **JUC-135** titrated with NB (a), 1,3-DNB (b), 2,4-DNT (c) and TNP (d) in DMF, respectively. The quenching efficiency (%) was estimated using the formula $(I_0\text{-}I)/I_0 \times 100\%$, where I_0 is the maximum fluorescence intensity of **JUC-135** before exposure to the analyte and I is the luminescent intensity for any given concentration of quencher.

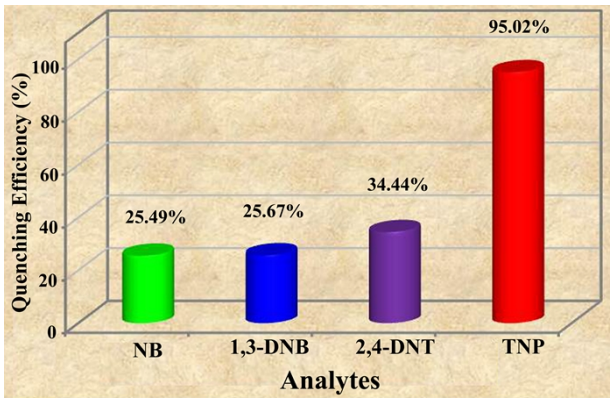

Fig. S6 Quenching efficiencies of **JUC-135** at 40 ppm for NB (green), 1,3-DNB (blue), 2,4-DNT (voilet) and TNP (red), respectively.

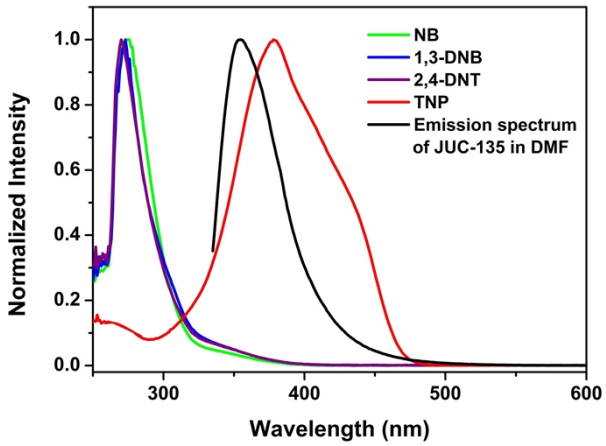

Fig. S7 Spectral overlap between the absorption spectra of analytes and the emission spectrum of **JUC-135** in DMF.

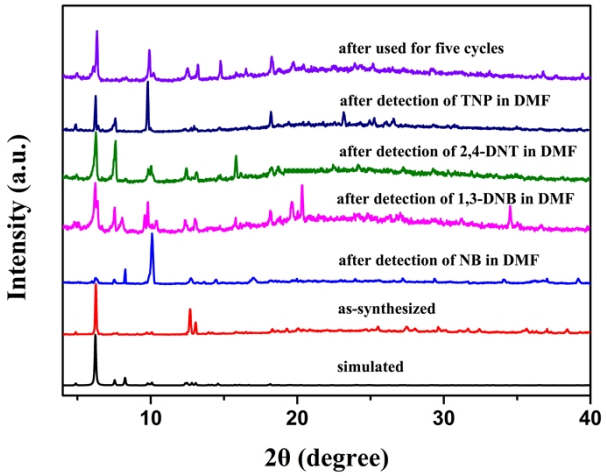

Fig. S8 PXRD patterns of **JUC-135** in different environments.

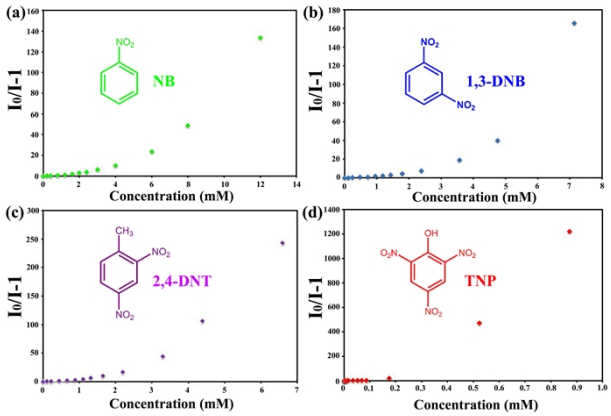

Fig. S9 Stern-Volmer plot for NB (a), 1,3-DNB (b), 2,4-DNT (c) and TNP (d) in full concentration region, respectively.

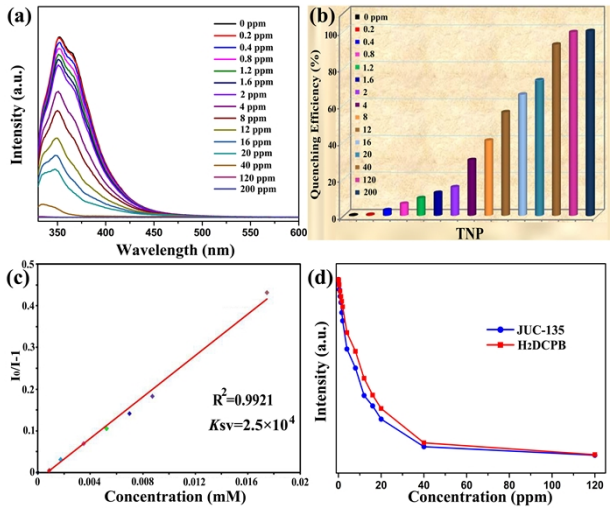

Fig. S10 The emission spectra of **H_2DCPB** (a) and corresponding quenching efficiency (b) titrated with TNP in DMF. (c) The Stern-Volmer plots for **H_2DCPB** with TNP in low concentration region. The solid lines represent fits to the concentration-resolved data using Stern-Volmer equation. (d) The relationships between emission intensity and different concentrations for TNP.

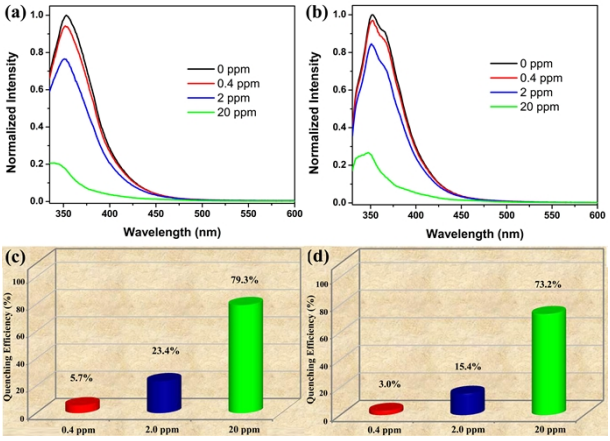

Fig. S11 The normalized intensity and and corresponding quenching efficiency of **JUC-135** (a, c) and **H_2DCPB** (b, d) in 0 ppm, 0.4 ppm, 2 ppm and 20 ppm TNP in DMF. **JUC-135** or **H_2DCPB** of 3.0 mg was dispersed in DMF of 3.0 ml.

Table S1 Selected bond lengths (Å) and angles (deg) for **JUC-135**.

JUC-135			
O(1)-Zn(1)	1.861(3)	O(2)-Zn(3)	1.972(4)
O(3)-Zn(1)	1.971(3)	O(4)-Zn(1)	1.972(3)
O(5)-Zn(1)#7	1.9510(16)	O(5)-Zn(1)	1.9511(16)
O(5)-Zn(1)#2	1.9513(16)	O(5)-Zn(3)	1.969(4)
O(6)-Zn(2)	1.988(2)	O(7)-Zn(2)#5	1.961(2)
O(8)-Zn(4)	1.954(3)	O(9)-Zn(2)	1.917(3)
O(10)-Zn(2)#8	1.9490(13)	O(10)-Zn(2)	1.9490(13)
O(10)-Zn(2)#5	1.9491(13)	O(10)-Zn(4)	1.955(4)
Zn(2)-O(7)#8	1.961(2)	Zn(3)-O(2)#2	1.972(4)
Zn(3)-O(2)#7	1.972(4)	Zn(4)-O(8)#8	1.954(3)
Zn(4)-O(8)#5	1.954(3)		
O(1)-Zn(1)-O(5)	116.69(16)	O(1)-Zn(1)-O(3)	105.49(12)
O(5)-Zn(1)-O(3)	115.87(9)	O(1)-Zn(1)-O(4)	110.06(16)
O(5)-Zn(1)-O(4)	109.13(11)	O(3)-Zn(1)-O(4)	97.97(14)
O(9)-Zn(2)-O(10)	109.65(16)	O(9)-Zn(2)-O(7)#8	117.50(17)
O(10)-Zn(2)-O(7)#8	109.74(11)	O(9)-Zn(2)-O(6)	105.52(12)
O(10)-Zn(2)-O(6)	112.41(9)	O(7)#8-Zn(2)-O(6)	101.78(13)
O(5)-Zn(3)-O(2)#2	99.51(14)	O(5)-Zn(3)-O(2)	99.52(14)
O(2)#2-Zn(3)-O(2)	117.33(8)	O(5)-Zn(3)-O(2)#7	99.51(14)
O(2)#2-Zn(3)-O(2)#7	117.32(8)	O(2)-Zn(3)-O(2)#7	117.32(8)
O(8)#8-Zn(4)-O(8)	104.86(14)	O(8)#8-Zn(4)-O(8)#5	104.86(14)
O(8)-Zn(4)-O(8)#5	104.85(14)	O(8)#8-Zn(4)-O(10)	113.77(12)
O(8)-Zn(4)-O(10)	113.77(12)	O(8)#5-Zn(4)-O(10)	113.76(12)

Symmetry transformations used to generate equivalent atoms:

#1 -y+1/3, -x+2/3, z+1/6 #2 -x+y, -x, z #3 -y+2/3, -x+1/3, z-1/6 #4 -x+y+2/3, y+1/3, z-1/6 #5 -y+1, x-y, z #6 -x+y+1/3, y-1/3, z+1/6 #7 -y, x-y, z #8 -x+y+1, -x+1, z